

Nuclear structure of light thallium isotopes as deduced from laser spectroscopy on a fast atom beam

J. A. Bounds*

The University of Tennessee, Knoxville, Tennessee 37996

C. R. Bingham

*The University of Tennessee, Knoxville, Tennessee 37996
and Oak Ridge National Laboratory, Oak Ridge, Tennessee 37831*

H. K. Carter, G. A. Leander, R. L. Mlekodaj,[†] and E. H. Spejewski[‡]
UNISOR, Oak Ridge Associated Universities, Oak Ridge, Tennessee 37831

W. M. Fairbank, Jr.

Colorado State University, Fort Collins, Colorado 80523

(Received 27 April 1987)

The neutron-deficient isotopes $^{189-194}\text{Tl}$ have been studied using collinear fast atom beam laser spectroscopy with mass-separated beams of 7×10^4 to 4×10^5 atoms per second. By laser excitation of the 535 nm atomic transitions of atoms in the beam, the $6s^2 7s^2 S_{1/2}$ and $6s^2 6p^2 P_{3/2}$ hyperfine structures were measured, as were the isotope shifts of the 535 nm transitions. From these, the magnetic dipole moments, spectroscopic quadrupole moments, and isotopic changes in mean-square charge radii were deduced. A large isomer shift in ^{193}Tl was observed, implying a larger deformation in the $\frac{9}{2}^-$ isomer than in the $\frac{1}{2}^+$ ground state. The $^{189,191,193}\text{Tl}^m$ isotopes have deformations that increase as the mass decreases. A deformed shell model calculation indicates that this increase in deformation can account for the drop in energy of the $\frac{9}{2}^-$ bandhead in these isotopes. An increase in neutron pairing correlations, having opposite and compensating effects on the rotational moment of inertia, maintains the spacing of the levels in the $\frac{9}{2}^-$ strong-coupled band. Results for $^{194}\text{Tl}^m$ differ from previously published values, but are consistent with the $^{190,192}\text{Tl}^m$ data.

INTRODUCTION

The mass region around Pb has been of particular interest to nuclear physicists due to the doubly-magic shell closures at ^{208}Pb . Nuclei near a closed proton or neutron shell can often be modeled by a single- or few-particle approximation. Thallium isotopes, with $Z=81$, have one less proton than the closed shell. The stable isotopes $^{203,205}\text{Tl}$ are known to have a ground-state nuclear spin of $\frac{1}{2}^+$, attributable to a single unpaired proton in a $3s_{1/2}$ orbital. This same ground-state spin has been detected or inferred both in the higher mass $^{207,209}\text{Tl}$ and in the lighter odd-mass Tl isotopes down to ^{185}Tl .¹ In all of these, the neutrons remain paired as their numbers change and thus do not influence the ground state spin. Higher energy states of $\frac{3}{2}^+$ and $\frac{5}{2}^+$ have been observed in most of these isotopes.² In addition, rotational bands built on a $1h_{9/2}$ state intruding across the $Z=82$ shell gap have been observed in the lighter isotopes. Nuclear spectroscopy has shown that the $\frac{9}{2}^-$ bandhead excitation energy above the ground state varies with mass number reaching a minimum at ^{189}Tl .^{2,3} In spite of this variation of energy, the rotational band spacings remain virtually constant throughout the isotopes. There have been several attempts to explain the decrease in excitation energy of the $\frac{9}{2}^-$ state.^{3,4} One simple explanation is that

nuclear deformation produces the lowering, but the constancy of the level spacings (or moment of inertia) in the band implies the deformation is not changing. Similar intruder states are known in Au, Hg, Pb, and Bi.⁵ The need for direct information concerning the deformations of the Tl isotopes prompted this work.

Since the nucleus of an atom interacts with the electrons of the atom, one way to study nuclei is to measure the hyperfine structure (hfs) of the electrons. The hfs perturbations to the electronic levels are produced by the magnetic and electric multipole moments of the nucleus and vary from isotope to isotope. In addition, the centers of gravity of the atomic levels shift between isotopes. In heavier atoms, this isotope shift (IS) is primarily due to the changes in the size (radius) and shape (deformation) of the nucleus. By measuring the hfs these properties of the nucleus may be deduced if a calculation of the electronic factor is possible, or if an experimental calibration exists to determine it. In earlier work hfs measurements have been made in Tl down to mass 194. This work takes advantage of collinear fast atom beam laser spectroscopy to observe the hfs of isotopes further from the region of stability.

EXPERIMENTAL METHOD

The experiments were performed at the University Isotope Separator at Oak Ridge (UNISOR) on-line to

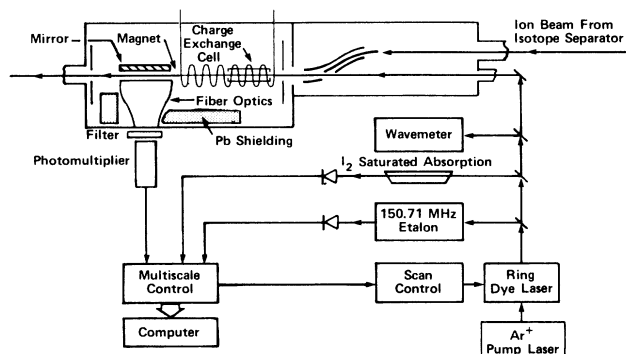


FIG. 1. Schematic of the UNISOR laser facility.

the Holifield Heavy Ion Research Facility (HHIRF). A schematic of the UNISOR laser facility is given in Fig. 1. A description of the experimental method used is given in Ref. 6. The laser frequency was scanned to excite transitions in the Tl atoms (Fig. 2) while holding all voltages constant. Through utilization of an efficient fiber optic collection device, a detection rate of one event per 1000 atoms in the beam was observed when the laser frequency coincided with the strongest ^{193}Tl spectral line. With this efficiency and typical noise rates observed during the experiments, it was essential to obtain a separator beam intensity exceeding 6×10^4 atoms/sec. Data were accumulated for one isotope at a time; an I_2 spectrum taken simultaneously with the data gave an absolute frequency reference. When operating on-line, positive identification of each mass was made by γ -ray spectroscopy of the beam deposits on a tape transport system. The short-lived Tl isotopes were produced via the $\text{Ta}(^{16}\text{O}, \text{xn})\text{Tl}$ reaction using stacked Ta foils in a high temperature ion source. Data were obtained on $^{189}\text{--}^{194}\text{Tl}$. For each isotope, wide laser scans were made to locate transitions, followed by scans of smaller regions to allow precise measurements of the hfs splittings. For demonstration purposes, the wider spectra obtained have been compressed to the same scale and are shown in relation to each other in Fig. 3. The average beam rate

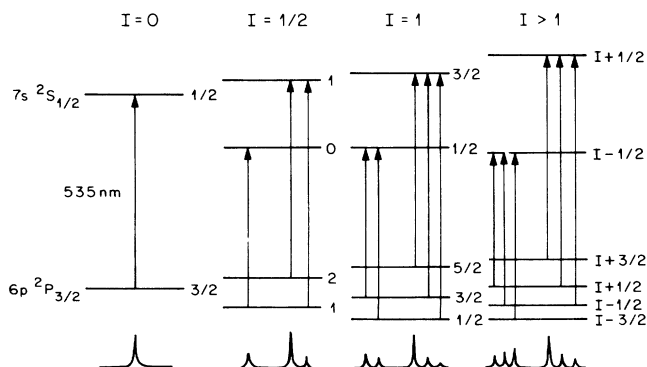


FIG. 2. Thallium hfs splitting for various nuclear spins I . Atomic terms are given at the left. Levels are numbered with their F values for the four possible cases of nuclear spin listed along the top. Allowed transitions and their normally ordered spectral patterns are shown. The hfs separations are not to scale.

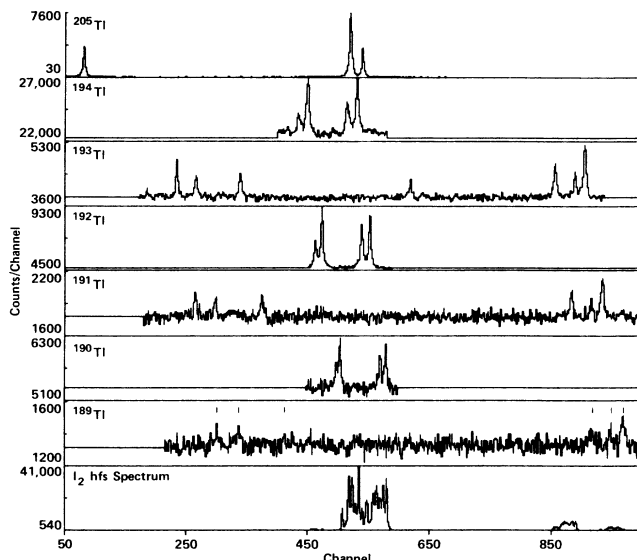


FIG. 3. Summed data sets for the Tl isotopes studied on line in comparison with the spectrum from ^{205}Tl at the same beam energies. The observed shifts in the centers of gravity of the Tl spectra are due to a combination of their isotope shifts and their different Doppler shifts.

and total time required to obtain the spectra in Fig. 3 are given in Table I. An expanded view of the ^{193}Tl data is given in Ref. 7 where the peaks are identified for both the $\frac{1}{2}^+$ ground state and the $\frac{9}{2}^-$ isomer. Only the isomeric state was observed for all of the other light Tl isotopes due to the preferential population of these states in heavy-ion reactions.

RESULTS AND DISCUSSION

The hyperfine structure observed arises from the splitting of the atomic terms as a result of interaction of the electrons with the dipole, quadrupole, and higher moments of the nuclear charge. The coupling of the nuclear and atomic angular momenta I and J determines the number of hyperfine lines in the spectra. The spacings of the observed peaks are related to the moments of the nucleus. For any spin greater than $1\hbar$, the Tl $6p^2P_{3/2}$ atomic J term is split into four F levels ($F=I+J$) whose spacings are given in terms of the hyperfine constants A , B , and C , related, respectively, to the dipole, quadrupole, and octupole moments of the nucleus.⁸ The spectral separations of peaks corresponding to transitions from the hfs levels F_1 and F_2 to a common F level in another J term are given by the classical formula⁹

TABLE I. Average beam rate and accumulation time for summed spectra shown in Fig. 3.

Mass	Half-time (min)	Average beam rate (sec) ⁻¹	Total time
194m	32.8	3.0×10^5	1 h 36 min
193m	2.1	3.5×10^5	3 h 10 min
192m	10.8	3.0×10^5	45 min
191m	5.2	1.8×10^5	50 min
190m	3.7	0.7×10^5	50 min
189m	1.4	0.9×10^5	51 min

$$W(F_2, F_1) = \frac{A}{2}(K_2 - K_1) + \frac{3B}{4} \frac{K_2(K_2 + 1) - K_1(K_1 + 1)}{2IJ(2I - 1)(2J - 1)} + \frac{5C}{4} \frac{(K_2^3 - K_1^3) + 4(K_2^2 - K_1^2) + \frac{4}{5}(K_2 - K_1)[-3IJ(I + 1)(J + 1) + I(I + 1) + J(J + 1) + 3]}{IJ(I - 1)(2I - 1)(J - 1)(2J - 1)}, \quad (1)$$

where

$$K_i = F_i(F_i + 1) - I(I + 1) - J(J + 1)$$

and $I > 1, J > 1$. The Tl $7s^2S_{1/2}$ term is split only by the dipole term since its $J = \frac{1}{2}$ will not couple to an observable higher multipole effect in the laboratory frame. The splittings of both J terms appear in the spectra. Peak identification is aided by two fundamental properties: (1) the ratio of dipole constants $A(7s^2S_{1/2})/A(6p^2P_{3/2})$ is relatively unchanging between isotopes (~ 46 for Tl) and (2) for $I > \frac{1}{2}$ there are necessarily two pairs of transitions having the same energy spacing (see Fig. 2). These features permitted unique peak assignments for all of the isotopes in spite of the unresolved doublets in the even mass spectra. Further confirmation of assignments was obtained by agreement of the observed peak intensities and profiles to those predicted by a mathematical model of the system.

The spectra were analyzed by least-squares fitting to the observed peak separations both with Eq. (1) and with the assumption that the octupole term was negligible. The values of the A and B constants for each isotope agreed for both fits; the C constant, when evaluated, was consistently within one standard deviation of zero.

Nonzero values of C have been measured in ^{127}I and ^{115}In using atomic-beam magnetic resonance (ABMR).^{9,10} These values, however, are considerably smaller than the resolution of the current experiment. For these reasons the values of C were assumed to be 0 MHz and results with just the A and B terms are reported here. For the even mass isomers, whose nuclear spins are not certain but believed to be $I = 7$, analysis was done for both spins 6 and 7 since these two nuclear spins give virtually identical atomic spectra. Table II lists the values of A and B obtained from the present measurements.

TI MAGNETIC DIPOLE MOMENTS

For a chain of isotopes, corresponding dipole constants A are known to be related by $[\mu/IA]_1 = [\mu/IA]_2(1 + \Delta_{12})$, where μ is the nuclear magnetic dipole moment and Δ_{12} , known as the hyperfine anomaly, corrects for the nucleus being nonpointlike. Ekstrom *et al.*^{15,16} have determined that this anomaly can be given approximately by

$$\Delta_{12} \sim \left(\frac{1 + \alpha_1/\mu_1}{1 + \alpha_2/\mu_2} \right) - 1$$

TABLE II. Tl hyperfine structure constants measured in the present experiment in comparison with the best previous results (in MHz).

Isomer	$A(7s^2S_{1/2})$	$A(6p^2P_{3/2})$	$B(6p^2P_{3/2})$	Comment
205g	12 292.4(8.3)	264.65(80)		
	12 291(15) ^a	265.038 273(2) ^b		
	12 284(6) ^c	264.35(75) ^c		
203g	12 179.7(5.6)	262.3(1.0)		
	12 184(15) ^a	262.029972(2) ^b		
	12 172(6) ^c	262.25(75) ^c		
201g	12 045.3(9.4)	255.0(5.0)		
	12 052(120) ^d	510(12) ^d		
194m	287.5(2.6)	5.4(1.8)	671(26)	If $I = 7$
	331.7(2.9)	6.9(2.0)	647(25)	If $I = 6$
193g	11 942(14)	259.9(7.0)		
193m	3263.0(2.4)	66.7(2.3)	-2476(20)	
192m	275.9(1.9)	5.8(1.0)	526(18)	If $I = 7$
	318.3(2.1)	7.2(1.3)	507(17)	If $I = 6$
191m	3225.9(3.4)	66.5(3.4)	-2562(31)	
190m	263.9(2.3)	5.4(1.6)	296(24)	If $I = 7$
	304.5(2.6)	6.6(1.8)	286(23)	If $I = 6$
189m	3204.5(4.8)	65.3(4.8)	-2578(44)	

^aReference 11.

^bReference 12.

^cReference 13.

^dReference 14.

TABLE III. Tl magnetic moments and isotope shifts of the 535 nm transition.

Isomer	μ (μ_N)	IS (GHz)	Isomer	μ (μ_N)	IS (GHz)
207g	1.876(5) ^a	1.783(3) ^a	198g	$\pm 0.00(1)^b$	-6.87(12) ^c
205m	0.41(5) ^d	—	197g	1.58(2) ^c	-7.02(12) ^c
205g	1.6382136(1) ^e	0.0 ^f	196m		-8.64(12) ^g
204m	1.187(6) ^h		196g	$\pm 0.07(1)^b$	
204g	$\pm 0.09(1)^b$	-1.08(12) ⁱ	195g	1.58(4) ^g	-8.22(12) ^g
203m	0.16(5) ^j		194m		-10.37(12) ^g
203g	1.6222569(1) ^e	-1.766(21) ^k		0.5397(49) ^l	-9.482(37) ^l ($I = 7$)
		-1.757(2) ^a		0.5313(47) ^l	-9.471(37) ^l ($I = 6$)
	1.6231(13) ^l	-1.758(18) ^l	194g	$\pm 0.14(1)^b$	
202m	0.896(42) ^m		193m	3.9482(39) ^l	-7.033(17) ^l
202g	$\pm 0.06(1)^b$	-3.12(12) ⁱ	193g	1.5912(22) ^l	-9.743(19) ^l
201g	1.61(2) ^j	-3.72(12) ⁱ	192m	0.5180(36) ^l	-10.892(30) ^l ($I = 7$)
	1.6051(17) ^l	-3.537(15) ^l		0.5121(34) ^l	-10.877(30) ^l ($I = 6$)
200g	$\pm 0.04(1)^b$	-5.07(12) ⁱ	191m	3.9034(48) ^l	-8.265(65) ^l
199g	1.60(2) ^b	-5.31(12) ⁱ	190m	0.4953(36) ^l	-12.286(65) ^l ($I = 7$)
198m	$\pm 0.64(7)^b$	-6.48(12) ⁿ		0.4900(42) ^l	-12.275(65) ^l ($I = 6$)
			189m	3.8776(63) ^l	-9.484(70) ^l

^aReference 13.^bReference 15.^cReference 17.^dReference 18.^eReference 15 which used the value from Ref. 19 with some corrections.^fAll isotope shifts listed here are given relative to ²⁰⁵Tl.^gReference 20.^hReference 21.ⁱReference 14.^jReference 22.^kReference 11.^lPresent work. The values for μ include the hfs anomaly but no errors due to it. Values for alternative spins are given for ^{190,192,194}Tl^m.^mReference 23.ⁿReference 24.

where, for the Tl $7s^2S_{1/2}$ term, $\alpha = \pm 0.01 \mu_N$ ($j_v = l \pm \frac{1}{2}$ or $j_p = l \mp \frac{1}{2}$; j, l describing the nuclear particle orbitals) based on similar values for gold. Knowing the magnetic dipole moment for the stable Tl isotopes, μ for the other isotopes was found using the above relations and the measured splittings of the $7s^2S_{1/2}$ term. All known magnetic dipole moments in the Tl isotope chain as well as the isotope shifts of the 535 nm line (to be discussed below) are given in Table III. These dipole moments, under the assumption that the spins of ^{190,192,194}Tl^m are 7^+ , are plotted in Fig. 4.

An interpretation of the moments down to mass 194 has been given by Ekstrom, Wannberg, and Shishodia.¹⁵ The spin $\frac{1}{2}$ moments of about $1.6 \mu_N$ are well below the Schmidt-limit value of $2.793 \mu_N$ for a single $3s_{1/2}$ proton orbital. Covello *et al.*²⁵, however, were able to derive such a value for the moments using calculations involving the intermediate coupling unified model by taking a spin gyromagnetic ratio $g_s \sim 0.62(g_s)_{\text{free}}$. The discontinuity at ²⁰⁷Tl has been attributed¹³ to a significant change in the contribution of configuration mixing due to the filling of the core-polarizing $vp_{1/2}$ hole between ²⁰⁵Tl and ²⁰⁷Tl and an expected decrease in the second-order effects from admixing with the $2^+ + \pi d_{3/2}$ configuration.

The most noticeable change in moments occurs for the spin 7 isomers. The variation of the moments with mass follow a smooth curve in Fig. 4, suggesting a common dominant configuration. (Note that the moment of ¹⁹⁴Tl^m, previously assumed to have a magnitude less than $0.089 \mu_N$ in the hfs measurements of Goorvitch, Davis,

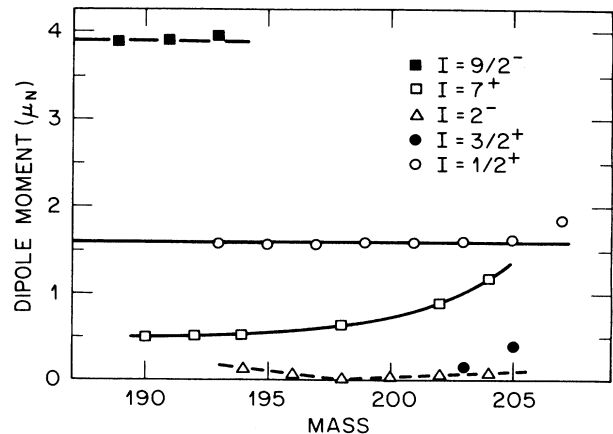


FIG. 4. Tl magnetic dipole moments. See Table III for data origins.

and Kleinman²⁰ and based on the paper by Brink²⁶ has been shown by this work to be in error). The obvious candidate for the dominant single-particle configuration is $\pi s_{1/2} \nu i_{13/2}$. The standard spherical shell model formulas for the magnetic moments²⁷

$$\mu = j[g_1 + (g_s - g_1)/(2l + 1)]$$

for one-particle configurations with $j = l + \frac{1}{2}$ and

$$\mu = \mu_1 + \mu_2$$

for two particle configurations with $I = j_1 + j_2$ will be used in the following discussion, since the spectroscopy of the odd Hg isotopes shows that the $i_{13/2}$ neutron remains largely decoupled from the deformation.²⁸ With $g_s/(g_s)_{\text{free}}$ of 0.5–0.6, the empirical values $\mu(\pi s_{1/2}) = 1.6 \mu_N$ and $\mu(\nu i_{13/2}) = -1.0 \mu_N$ are reproduced. Our measured values $\mu(7^+) = 0.6 \mu_N$ for the light Tl isotopes are then also reproduced. Since the empirical $\frac{1}{2}^+$ moments are constant for odd Tl isotopes with $N \leq 124$ (Fig. 4), and the empirical $\frac{13}{2}^+$ moments are almost constant for Hg, Pb, and Po isotopes with $N < 124$,²⁹ the variation of the 7^+ moments are remarkable. Hashimoto *et al.*^{23,30} attribute the elevated moment of ²⁰²Tl to a modest admixture of $\pi h_{11/2} \nu p_{3/2}$ in the wave function. It would then appear that the configuration mixing decreases in the lighter and more deformed isotopes. Alternatively, one could surmise that an increasing admixture of $\pi d_{3/2} \nu i_{13/2}$ could lower the magnetic moments of the lighter isotopes. Certainly deformation mixes the $\pi s_{1/2}$ and $d_{3/2}$ orbits, and $\langle S_2 \rangle$ for the $\Omega = \frac{1}{2}$ orbital is reduced from 0.5 for spherical shape to 0.4 at $\beta_2 = -0.15$, but if this explanation were correct it is hard to understand why the $\frac{1}{2}^+$ moment of the odd-mass Tl isotopes would remain constant. A factor could be that the decoupled $\nu i_{13/2}$ orbit polarizes the nucleus to oblate shape³¹ where the $s_{1/2}$ - $d_{3/2}$ interaction is strongest. Taken at face value, however, the measured moments appear to imply that the dominant shell model configuration is purer for the more deformed isotopes.

Neither spin $\frac{3}{2}^+$ excited states nor spin 2^- isomers were seen in the new data due to their absence or paucity in the separator beam. Moments for the excited $\frac{3}{2}^+$ states have been measured only for ^{203,205}Tl where they were excited by bombarding natural Tl with electrons.^{18,22} The $\frac{3}{2}^+$ moments indicate small admixing of other configurations with the $\pi d_{3/2}$ configuration which has a Schmidt limit of $0.13 \mu_N$. The moments of the 2^- states, measured by ABMR, are believed to change almost linearly from negative to positive as the Tl-isotope

mass decreases.¹⁵ The likely origin of this is a changing mixture of the configurations $2^-(\pi s_{1/2} \nu f_{5/2})$ and $2^-(\pi s_{1/2} \nu p_{3/2})$ with a possible contribution from $2^-(\pi d_{3/2} \nu p_{1/2})$ as the first two configurations vie for dominance.

The newest addition to the dipole moment measurements are the three spin $\frac{9}{2}$ values from this work. These moments are very similar to other spin $\frac{9}{2}$ moments in the neighboring regions of the chart of the nuclides and are a result of a $\pi h_{9/2}$ configuration. The values of the Tl moments are about $3.9 \mu_N$, well within the Schmidt limits for a $j = \frac{9}{2}$ nucleus which are $2.63 \mu_N$ for $j = l - \frac{1}{2}$ and $6.79 \mu_N$ for $j = l + \frac{1}{2}$.

Tl ELECTRIC QUADRUPOLE MOMENTS

No previously measured quadrupole moments are known for Tl, so no calibration exists to extract the moment from the hyperfine constant B . The screening electrons and relativistic correction factors prevent an accurate simple calculation of the electronic factor relating B and Q , but complex calculations using a relativistic Hartree-Fock approach and an optimized Hartree-Fock-Slater method have been done by Lindgren and Rosen.³² Taking from those calculations an approximate value of $\langle r^{-3} \rangle_{02} \approx 12$, the relation obtained between the spectroscopic quadrupole moment Q_s and B is $Q_s = (8.9 \times 10^{-4} \text{ b/MHz})B$. Other methods give values of Q_s which vary by $\mp 10\%$ from the values obtained here.³³ The Sternheimer correction for screening electrons is difficult to calculate accurately for Tl (Ref. 8) and is not included in these calculations. Its effect would be only to scale the magnitudes of the moments without changing their relative sizes. The Q_s value obtained in this manner and listed in Table IV may be either too large or too small but are proportionally correct. The error range shown reflects only the measurement uncertainty; for absolute quadrupole moment values a conservative error range of 20% should be assumed.

The moments in the even-mass Tl isotopes result from the coupling of an odd proton and an odd neutron and so are not connected by simple relations with the intrinsic quadrupole moments Q_0 . Assuming the moments are proportional to the B 's, there is a large change in going from ¹⁹⁴Tl^m to ¹⁹⁰Tl^m. This change shows up as a reduced spacing of the peaks in the even-mass data of Fig. 3. The actual values of these moments are not estimated here.

For the $\frac{9}{2}^-$ nuclei, the well-known relation for axially

TABLE IV. Moments and deformations of light Tl isotopes.

Isomer	Q_s (e b)	Q_0 (e b)	β_2 from Q_0	$\langle \beta_2^2 \rangle^{1/2}$ from isotope shift
193g				0.099(1)
193m	-2.20(2)	-4.04(3)	-0.144(1)	0.158(1)
191m	-2.28(3)	-4.18(5)	-0.151(2)	0.170(2)
189m	-2.29(4)	-4.21(7)	-0.153(3)	0.181(2)

symmetric deformation and strong coupling of the odd proton³⁴

$$Q_s = Q_0 \frac{3K^2 - I(I+1)}{(I+1)(2I+3)}$$

has been used to give the Q_0 values in Table IV. The strong-coupled character of the $h_{9/2}$ band suggests predominantly oblate deformation; hence $I = \frac{9}{2}$ and $K = \frac{9}{2}$, giving negative values of Q_0 . Assuming an axially symmetric ellipsoid, the nuclear deformations β_2 can be derived from the expression³⁵

$$Q_0 = \frac{2ZA^{2/3}r_0^2\beta_2(1+0.36\beta_2)}{(5\pi)^{1/2}}$$

and are also tabulated. The relationship of the deformation parameter β_2 and other quadrupole deformation parameters is also given in Ref. 35. A quite important feature to come out of the present calculations is that even though the absolute scale for the quadrupole moments is unknown, there is an observable trend of increasing deformation in going away from stability. This point is addressed further in the discussion below.

TI ISOTOPE SHIFTS

The isotope shifts, the changes in the centers of gravity of the transitional frequencies from one isotope to the next, yield information concerning sizes and shapes of nuclei. Values for all known isotope shifts for the 535 nm transition in Tl are given in Table III. It can be seen that the values from the present work are consistent with previous measurements. With the exceptions of ^{203,205,207}Tl, the isotope shifts measured here are more precise than previous optical measurements by a factor of from 2 to 6. This improvement is attributable to the linewidths in these collinear laser experiments (~60–150 MHz) as compared to the previous optical experiments which used lamps as the light sources and which had corresponding Doppler widths of ~0.9–1.5 GHz.

The isotope shift is composed of a field shift due to volume changes and a mass shift due to a difference in isotopic mass.³⁶ The mass shift in turn is composed of a normal (NMS) and specific (SMS) mass shift. For the Tl 535 nm line, the NMS is only ~8 MHz for adjacent isotopes. Arising from electron correlations, the SMS cannot be readily calculated, but for Pb it has been estimated that the SMS equals (0 ± 10) NMS (Ref. 37) and for Hg SMS equals (0 ± 0.5) NMS.³⁸ The value (0 ± 1) NMS was chosen for the Tl data based on the arguments of Heilig and Steudel.³⁹ After determining the centers of gravity and correcting for the Doppler shifts in the current data, subtracting the calculated mass shifts yielded the field shifts. A variety of expressions relating the field shifts to nuclear radial moments have appeared in the literature; nearly all of them predict a product of electronic and nuclear factors. Taking Seltzer's⁴⁰ values for the nuclear component of the field shifts gives

$$\lambda = \langle r^2 \rangle - 0.0111 \langle r^4 \rangle + 2.936 \times 10^{-6} \langle r^6 \rangle + \dots,$$

where λ times an electronic factor gives the field shift. Assuming a deformed radius $r_d = r_b(1 + \beta Y_{20})$, where β is the deformation parameter and r_b is chosen to make the nuclear volume equal to that of a sphere of radius $r_0 A^{1/3}$, it can be shown that for Tl

$$\lambda \sim 0.93 \langle r^2 \rangle_A + 0.89 \langle r^2 \rangle_\beta, \quad (2)$$

where A and β refer to mass-only and deformation-only changes in mean-square radii. This agrees with formulas used by Thompson *et al.*³⁷ for Pb and by Bonn *et al.*³⁸ for Hg.

As with most other electronic constants in Tl, the proportionality factor between the field shift and λ is not accurately calculable due to screening electrons. Having no certain calibrations for the electronic factor, various normalizations were investigated. Muonic x-ray data and electron scattering data give the moments $\langle r^k e^{-ar} \rangle$, not differences in radial moments, but a model dependent value of $-0.115(3)$ fm² for the ^{203,205}Tl isotope shift may be obtained.⁴¹ Assuming negligible higher moments, an electronic factor of 15.16(43) GHz/fm² is deduced. Droplet model predictions⁴² give the ^{203,205}Tl shift to be 0.106(10) fm² and thus the electronic factor would be 16.4(1.6) GHz/fm². If the muonic atom data were used for calibration, a plot of $\langle r^2 \rangle$ for the Tl isotopes would have data points which for the most part would fall about one-fourth of the way between the predictions of the droplet model and the values of $\langle r^2 \rangle$ obtained from calculations for a spherical nucleus having radius $r_0 A^{1/3}$. Such a plot for Pb is given by Thompson *et al.*³⁷ However, both the droplet model and Eq. (2) indicate that points should lie on or above the droplet model $\beta=0$ line. By normalizing the droplet model predictions to the measured field shifts, estimates of the nuclear deformations were obtained. Since ²⁰⁷Tl is only one proton away from a doubly closed shell, the assumption was made that it has a deformation of zero. The electronic factor was chosen to make the $\beta=0$ droplet model prediction for the field shifts pass through the ²⁰⁷Tl point and be below or on the experimental values for all the other isotopes. Figure 5 shows the results of this normalization. Note that with this normalization the point for ²⁰⁰Tl also falls on the $\beta=0$ prediction. Lines obtained for nonzero deformations are included. There is considerable odd-even staggering in the data. As with the quadrupole moment data, an increase in deformation in going away from stability is observed. Deformations obtained for the $\frac{9}{2}^-$ isomers are included in Table IV. Agreement in the deformations obtained from the isotope shifts and from the quadrupole moments is very good considering the assumptions made and considering also that the quadrupole moment gives $\langle \beta \rangle$ while the isotope shift gives $\delta \langle \beta^2 \rangle$. A disagreement in derived values similar to those here has previously been observed in the neutron-deficient Hg isotopes,³⁸ where it is believed that Q_0 is underestimated from Q_s because of violation of strong coupling and axial symmetry. We have checked this explanation for the case of ¹⁹¹Tl by a model calculation in which a triaxial rotor is coupled to a quasiparticle in the corresponding triaxial Woods-

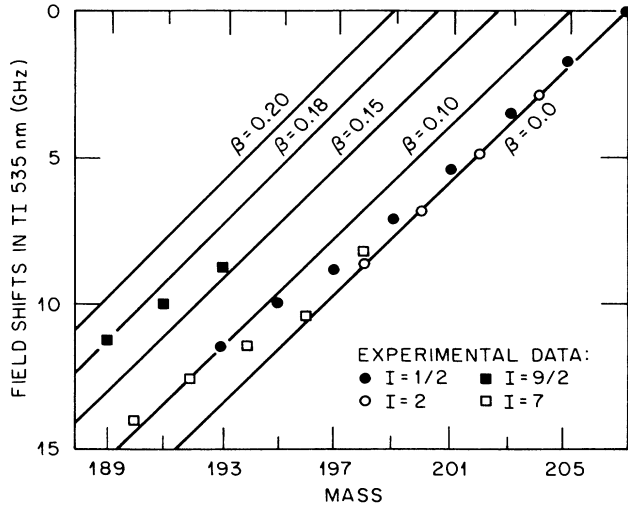


FIG. 5. Tl 535 nm field shifts. The field shifts (shown as points) are derived from the isotope shifts listed in Table III. Predictions of the deformed droplet model, calculated for various deformations and normalized to masses 200 and 207, are given as lines.

Saxon potential. Setting $\beta_2=0.16$, the spacing of the $\frac{9}{2}^-$ and $\frac{11}{2}^-$ levels is reproduced with the core moment of inertia corresponding to $E(2_1^+)=250$ keV, and the position of the $\frac{13}{2}^-$ level (i.e., the signature splitting) is reproduced with the triaxiality parameter $\gamma=39^\circ$. The resulting Q_s for the $\frac{9}{2}^-$ level is 6% lower than the value for strong coupling to an axially symmetric core with $\beta_2=0.16$, $\gamma=60^\circ$. Since $\langle r^2 \rangle$ is very weakly dependent on γ , this accounts for one-half of the difference between the β_2 values from the quadrupole moment and the isotope shift. The differences in Tl are larger for the lighter isotopes and may be in part due to mixing with a coexisting state of opposite and larger deformation, which could simultaneously reduce the quadrupole moment and increase the effective radius.

The assumption of zero deformation for ^{200}Tl in normalizing the droplet model calculations to the data results in predictions with smaller slopes than if ^{200}Tl were assumed to have a nonzero deformation. Thus, it is likely that the lines in Fig. 5 represent minimum slopes and that deformations obtained by reading the plot are minimum values. Regardless of actual values, the plot shows that in going away from the closed shell of ^{207}Tl the deformations are increasing. Similarly increasing deformations in going away from the shell closure have been deduced in Au,⁴³ Hg,³⁸ and Pb.³⁷ The deformations for each nuclear spin are in general smoothly changing. Furthermore, the isomer shift in ^{193}Tl can be interpreted as a large change in deformation between the ground and excited states, a change of as much as 60% if the normalization is correct. There is remarkable similarity in the relative isotope shifts in the Pb region. Comparisons of the shifts in Os, Pt, Au, Hg, Tl, and Pb appear in the article by Strieb *et al.*⁴³ but perhaps more strikingly in the article by Barboza-Flores, Redi, and Stroke.⁴⁴ The latter article compares Hg, Tl, Pb, Bi, and Fr isotope shifts normalized to the shift between the iso-

topes with neutron numbers 122 and 124. Figure 2 in their article can be expanded with the new $^{189-194}\text{Tl}$ data of this work and the extended $^{196-214}\text{Pb}$ data of Anselment *et al.*⁴⁵ The addition of a proton from one isotope chain to the next causes virtually no change in relative isotope shifts.

The remeasurement of the $^{194}\text{Tl}^m$ isotope shift in the present work resulted in a somewhat higher value than previously obtained.²⁰ The new value is in better agreement with an extrapolation of the $^{198,200,202,204}\text{Tl}$ data and shows better similarity to the Hg data. From the description of the data analysis in the previous $^{194,195,196}\text{Tl}$ experiment,²⁰ it is reasonable to expect that a reanalysis of the old data with the new values for ^{194}Tl could alter the derived isotope shifts for $^{195,196}\text{Tl}$ bringing them closer to the pattern prevalent in this mass region. The shifts of $^{189,191,193}\text{Tl}$, being $\frac{9}{2}^-$ isomers, show a new pattern since they do not correspond to other neighboring isotones having a different number of protons.

THEORETICAL INTERPRETATION

A calculation was carried out to see if all of the observed features of the Tl isotopes would emerge from the deformed shell model. Details and results of the calculation were first presented in Ref. 7. The deformations deduced from the present measurements were shown to be sufficient to account for the mass dependence of the $\frac{9}{2}^-$ excitation energy. The upturn in the $\frac{9}{2}^-$ energy in the lightest Tl isotopes also was reproduced in the calculation owing to the difference in rate at which the Strutinsky shell corrections change with mass at the respective deformations of the $\frac{1}{2}^+$ and $\frac{9}{2}^-$ configurations. Rotational excitation energies for $^{185-199}\text{Tl}$ are also reproduced by the calculation. Whereas it was previously thought that a simple correspondence existed between deformation and the rotational moment of inertia, both changing deformation and the presence of nearly constant strongly-coupled bands based on the $\frac{9}{2}^-$ level in the Tl isotopes indicate that the relationship is more complex. The calculation suggests that when the number of valence neutron holes increases, both the deformation and the neutron-pairing correlations increase with opposite and compensating effects on the moment of inertia, producing the experimentally observed features.

While the deformed shell model has reproduced all the observed features, it may be possible that other models could do as well. Krygin and Mitroshin⁴⁶ interpreted the large isotope shifts in the Hg data in terms of an increase of the effective charge on the nuclear surface rather than in terms of a deformation change. Due to similarities in this mass region it may be possible that such a model could be applied to the Tl isotope shift data as well. Nevertheless, as pointed out earlier the sizes of the quadrupole moments and their changes with decreasing A tends to confirm the interpretation in terms of a larger deformation for the intruder $h_{9/2}$ level and its variation with mass number.

SUMMARY

Isotope shifts and magnetic dipole moment measurements have been extended away from stability to $^{189}\text{Tl}^m$.

Estimates of electric quadrupole moments and nuclear deformations show an increase in deformation as A is decreased away from stability. The changing deformation occurs despite the constant moment of inertia, revealing the fallacy of assuming that a constant moment of inertia implies a constant deformation. An interesting aspect of the competition between quadrupole and pairing correlations has been demonstrated, offering insight into the properties observed not only in Tl but in neighboring masses as well, potentially being applicable to many parts of the chart of the nuclides.

ACKNOWLEDGMENTS

The authors wish to thank C. E. Bemis, Jr., J. L. Wood, and E. F. Zganjar for many helpful suggestions

concerning the design and construction of the laser facility and the need for these measurements, C. E. Ekstrom and E. W. Otten for valuable comments on the interpretation of the data, C. A. Reed and C. N. Thomas for their technical aid, and the Holifield Heavy Ion Research Facility operations staff for delivering the intense ion beams required for these experiments. This work was supported in part by the U.S. Department of Energy under Contract No. DE-AS05-76ER04936 (UTK), No. DE-AC05-76OR00033 (UNISOR), and No. DE-AC05-84OR21400 (ORNL) and supported in part by Vanderbilt University, Nashville, TN, through a U.S. Department of Energy Contract No. DE-AS-05-76ER05034.

*Present address: Los Alamos National Laboratory, Mail Stop D449, Los Alamos, NM 87545.

†Present address: Oak Ridge National Laboratory, Oak Ridge, TN 37831.

‡Present address: Special Projects Division, Oak Ridge Associated Universities, Oak Ridge, TN 37831.

¹Y. A. Ellis-Akovi, Nucl. Data Sheets **33**, 557 (1981).

²J. O. Newton, S. D. Cirilov, F. S. Stephens, and R. M. Diamond, Nucl. Phys. **A148**, 593 (1970); A. G. Schmidt, R. L. Mlekodaj, R. L. Robinson, F. T. Avignone, J. Lin, G. M. Gowdy, J. L. Wood, and R. W. Fink, Phys. Lett. **66B**, 133 (1977); A. H. Kahler, Ph. D. thesis, University of Tennessee, 1978.

³E. Coenen, K. Deneffe, M. Huyse, and P. Van Duppen, in *Proceedings of the Seventh International Conference on Atomic Masses and Fundamental Constants, Darmstadt, 1984*, edited by O. Klepper (Technische Hochschule, Darmstadt, 1984).

⁴R. M. Diamond and F. S. Stephens, Nucl. Phys. **45**, 632 (1963); A. L. Goodman, Nucl. Phys. **A287**, 1 (1977).

⁵K. Heyde, P. Van Isacker, M. Waroquier, J. L. Wood, and R. A. Meyer, Phys. Rep. **102**, 291 (1983).

⁶C. R. Bingham, J. A. Bounds, H. K. Carter, R. L. Mlekodaj, J. C. Griffin, and W. M. Fairbank, Jr., Nucl. Instrum. Methods Phys. Res. B **26**, 426 (1987).

⁷J. A. Bounds, C. R. Bingham, P. Juncar, H. K. Carter, G. A. Leander, R. L. Mlekodaj, E. H. Spejewski, and W. M. Fairbank, Jr., Phys. Rev. Lett. **55**, 2269 (1985).

⁸C. Schwartz, Phys. Rev. **105**, 173 (1957).

⁹V. Jaccarino, J. G. King, R. A. Satten, and H. H. Stroke, Phys. Rev. **94**, 1798 (1954).

¹⁰P. Kusch and T. G. Eck, Phys. Rev. **94**, 1799 (1954).

¹¹A. I. Odinstov, Opt. Spektrosk. **9**, 137 (1960) [Opt. Spectrosc. (USSR) **9**, 75 (1960)].

¹²F. R. Petersen, H. G. Palmer, and J. H. Shirley, Bull. Am. Phys. Soc. **51**, 1203 (1968).

¹³R. Neugart, H. H. Stroke, S. A. Ahmad, H. T. Duong, H. L. Ravn, and K. Wendt, Phys. Rev. Lett. **55**, 1559 (1985).

¹⁴R. J. Hull and H. H. Stroke, Phys. Rev. **122**, 1574 (1961).

¹⁵C. Ekstrom, G. Wannberg, and Y. S. Shishodia, Hyp. Inter. **1**, 437 (1976).

¹⁶C. Ekstrom, L. Robertsson, S. Ingelman, G. Wannberg, I. Ragnarsson, and the ISOLDE collaboration, Nucl. Phys. **A348**, 25 (1980).

¹⁷S. P. Davis, H. Kleiman, D. Goorvitch, and T. Aung, J. Opt. Soc. Am. **56**, 1604 (1966).

¹⁸M. Y. Chen, S. C. Cheng, W. Y. Lee, A. M. Rushton, and C. S. Wu, Nucl. Phys. **A181**, 25 (1972).

¹⁹E. B. Baker and L. W. Burd, Rev. Sci. Instrum. **34**, 238 (1963).

²⁰D. Goorvitch, S. P. Davis, and H. Kleiman, Phys. Rev. **188**, 1897 (1969).

²¹K. H. Maier, Nucl. Phys. **A195**, 577 (1972).

²²E. Karlsson, E. Matthias, S. Gustafsson, K. Johansson, A. G. Svensson, S. Ogaza, and P. da Rocha Andrade, Nucl. Phys. **61**, 582 (1965).

²³O. Hashimoto, A. Sumi, T. Nomura, S. Nagamiya, K. Nakai, T. Yamazaki, and K. Miyano, Nucl. Phys. **A218**, 180 (1974).

²⁴D. Goorvitch, H. Kleiman, and S. P. Davis, Nucl. Phys. **A99**, 1 (1967).

²⁵A. Covello and G. Sartoris, Nucl. Phys. **A93**, 481 (1967); N. Azzis and A. Covello, *ibid.* **A123**, 681 (1969).

²⁶G. O. Brink, J. C. Hubbs, W. A. Nierenberg, and J. L. Worcester, Phys. Rev. **107**, 189 (1957).

²⁷A. de Shalit and I. Talmi, *Nuclear Shell Theory* (Academic, New York, 1963).

²⁸*Table of Isotopes*, edited by C. M. Lederer and V. S. Shirley (Wiley, New York, 1978).

²⁹P. Dabkiewicz, F. Buchinger, H. Fischer, H.-J. Kluge, H. Kremmling, T. Kühl, A. C. Müller, and H. A. Schuessler, Phys. Lett. **82B**, 199 (1979).

³⁰O. Hashimoto, A. Sumi, T. Nomura, S. Nagamiya, K. Nakai, T. Yamazaki, and K. Miyano, Suppl. J. Phys. Soc. Jpn. **34**, S269 (1973).

³¹I. Ragnarsson, in *Future Directions in Studies of Nuclei Far From Nuclei*, edited by J. H. Hamilton, E. H. Spejewski, C. R. Bingham, and E. F. Zganjar (North-Holland, Amsterdam, 1980), p. 367.

³²I. Lindgren and A. Rosen, Case Studies At. Coll. Phys. **4**, 93 (1975).

³³E. W. Otten, private communication.

³⁴A. Bohr and B. R. Mottelson, *Nuclear Structure* (Benjamin, London, 1975), Vol. 2.

³⁵K. E. G. Löbner, M. Vetter, and V. Hönl, Nucl. Data Tables A **7**, 495 (1970).

³⁶W. H. King, *Isotope Shifts in Atomic Spectra* (Plenum, New York, 1984).

³⁷R. C. Thompson, M. Anselment, K. Bekk, S. Göring, A.

- Hanser, G. Meisel, H. Rebel, G. Schatz, and B. A. Brown, *J. Phys. G* **9**, 443 (1983).
- ³⁸J. Bonn, G. Huber, H.-J. Kluge, and E. W. Otten, *Z. Phys. A* **276**, 203 (1976); T. Kühl, P. Dabkiewicz, C. Duke, H. Fischer, H.-J. Kluge, H. Kremmling, and E.-W. Otten, *Phys. Rev. Lett.* **39**, 180 (1977); G. Ulm, S. K. Bhattacharjee, P. Dabkiewicz, G. Huber, H.-K. Kluge, T. Kühl, H. Lochmann, E.-W. Otten, K. Wendt, S. A. Ahmad, W. Klempt, R. Neugart, and the ISOLDE collaboration, *Z. Phys.* **325**, 247 (1986).
- ³⁹K. Heilig and A. Steudel, *At. Data Nucl. Data Tables* **14**, 613 (1974).
- ⁴⁰E. C. Seltzer, *Phys. Rev.* **188**, 1916 (1969).
- ⁴¹R. Engfer, H. Schneuwly, J. L. Vuilleumier, H. K. Walter, and A. Zehnder, *At. Data Nucl. Data Tables* **14**, 509 (1974).
- ⁴²W. D. Myers and K.-H. Schmidt, *Nucl. Phys.* **A410**, 61 (1983).
- ⁴³J. Streib, H.-J. Kluge, H. Kremmling, R. B. Moore, H. W. Schaaf, and K. Wallmeroth, *Z. Phys. A* **321**, 537 (1985).
- ⁴⁴M. Barboza-Flores, O. Redi, and H. H. Stroke, *Z. Phys. A* **321**, 85 (1985).
- ⁴⁵M. Anselment, W. Faubel, S. Göring, A. Hanser, G. Meisel, H. Rebel, and G. Schatz, *Nucl. Phys. A* **451**, 471 (1986).
- ⁴⁶G. B. Krygin and V. E. Mitroshin, *Yad, Fiz.* **41**, 304 (1985); *Fiz. Elem. Chastits At. Yadra* **16**, 927 (1985).